

CREATING POSTERS USING POWERPOINT

Ian Levstein, MS
Forensic Science Center
Updated, Fall 2013

Why a Poster?

- ▣ A poster is your opportunity to
 - make one point → loudly and clearly
 - stimulate interest and discussion
 - receive feedback on research

- ▣ A poster is not
 - a research paper stuck to a board

Poster Size

- ▣ Largest size slide that Powerpoint can create is 56" x 56"

Display Board Size:	Optimum Powerpoint Slide Size:
None (free hanging)	56" x 56"
72" x 48"	56" x 46"
48" x 36"	46" x 34"

Poster Size (cont.)

- ▣ Do not *ever* create a poster that exceeds the size of the slide
 - easy to do if you're not careful
- ▣ Doing so will initiate an unfortunate chain of events if/when converting to a PDF file

Transporting

- ▣ For auto/train:
 - poster tubes usually up to 36"
- ▣ For airplane:
 - PVC pipe with 2 end caps
- ▣ Don't leave the poster in your car!
- ▣ Know the phone number of the last person leaving for the airport

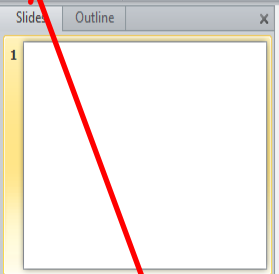
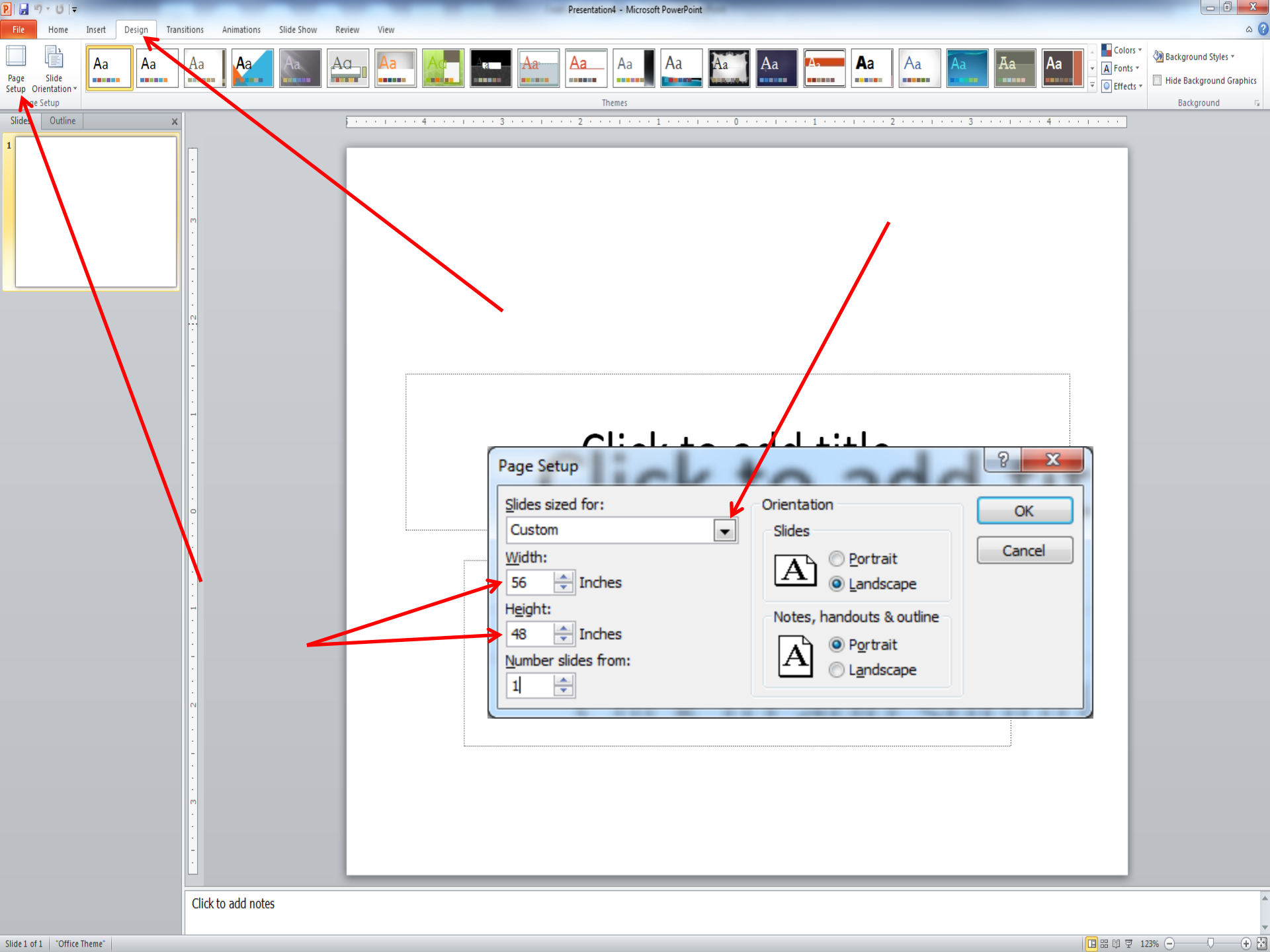
Administrative

- ▣ Find out in advance what the business needs in order to print successfully:
 - how much lead time do they need?
 - what version of Powerpoint do they use?
 - ▣ compatibility issues between versions?
 - ▣ what about reprints?
 - what are their business hours?
 - ▣ can they print on short notice if required?
 - do they trim the posters?



Getting Started

- ▣ You are going to create a single, large slide
- ▣ Start Powerpoint
 - create a new, blank slide
 - delete any existing text boxes
- ▣ Design → Page Setup
- ▣ Change width to 56" and height to 48" (or size of your choice), click OK



Page Setup

Slides sized for: Custom

Width: 56 Inches

Height: 48 Inches

Number slides from: 1

Orientation

Slides

Portrait

Landscape

Notes, handouts & outline

Portrait

Landscape

OK Cancel

Click to add notes

Getting Started (cont.)

- ▣ Use built-in rulers/ grids (View → Ruler)
- ▣ Most commercial large-format printers require a 2" margin on right hand side
- ▣ Allow lots of time to create

Text

- ▣ Text should already exist
 - don't try to edit and compose at the same time
 - several small text boxes are better than a single large one
 - can be resized
 - can be justified

- ▣ Be consistent
 - be consistent
 - ▣ be consistent

Images

- ▣ GIFs or TIFFs
 - uncompressed
 - even low quality images look good when large

- ▣ JPGs
 - compressed
 - low quality images look pixilated when enlarged
 - high resolution images may be okay

Images (cont.)

This is fine:



<http://www.flickr.com/photos/obiwanjr/838737075/>

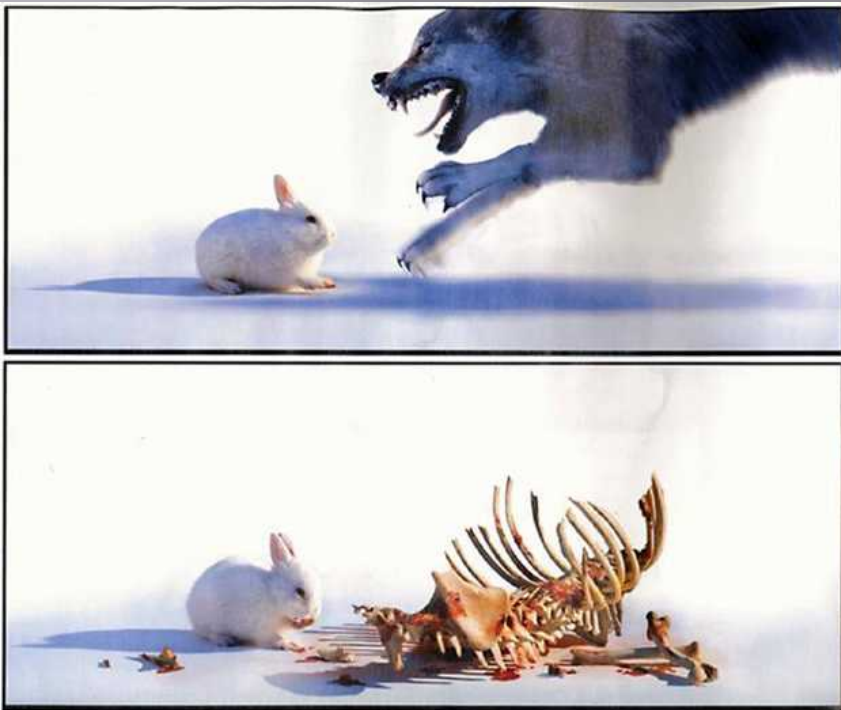
2"

This is
not:

Picture will
compress
and/or text
will scroll



2" margin on right is critical
Left margin is less critical



<http://tvtropes.org/pmwiki/pmwiki.php/Main/KillerRabbit>

Images (cont.)

- It's easy to add a 2" margin to your poster
- create a new slide 2" wider
- copy/paste from one slide to the other



Internal Validation of GeneMapper[®]ID-X for use in Forensic Casework

Former Student, BS¹; Colleague A, MFS²; Colleague B, MS³; Colleague C, MS⁴; Head Honcho, PhD⁵
¹Marshall University, Forensic Science Department, 1401 Forensic Science Dr., Huntington, WV 25701
²Palm Beach County Sheriff's Office, Forensic Biology Unit, 3228 Gun Club Rd., West Palm Beach, FL 33406



ABSTRACT

Due to the implementation of robotic equipment to extract, quantify, amplify, and detect forensic DNA samples, the bottleneck of forensic DNA analysis has shifted to data interpretation. There is now a need for computer software that maximizes efficiency and minimizes the resources needed for DNA analysis. Applied Biosystems' GeneMapper[®]ID-X is one of the software systems capable of reducing this bottleneck and providing a suite of tools to assist in single source and DNA mixture interpretation. GeneMapper[®]ID-X v12 (GMD-X) was validated for use with questioned casework samples and a foundation to utilize the expert system capabilities for known casework samples was established. Original GeneMapper[®]ID v3.1 (GMD) validation data was analyzed with GMD-X and the results were compared. The GMD-X software was able to produce accurate, reliable, reproducible and concordant results to those obtained using GMD. It was also the goal of this project to find a software system that can aid in performing interpretation of DNA mixtures. Therefore, the mixture deconvolution tool portions of both GMD-X and Nicholson Forensics, LLC's ArmaDeQ[™] were evaluated for their use in deconvoluting two and three-person DNA mixtures.

RESULTS AND DISCUSSION

Known Samples and Stratter Studies

- Known samples were concordant for 29/31 known samples compared to the data analyzed using GMD
- The first non-concordance could be attributed to a lower calling threshold, while the second was due to a failure in Size Quality
- Generally, the recommended stutter %s for PFSO with GMD-X were less than those published by PowerGen

Sensitivity and Analytical Threshold Studies

- 3100-A PFR kit below 10% with greater frequency at $40-120pg$ for all three reagent times and at three sample sets
- 3100-B PFR kit below 10% with greater frequency at $40-120pg$ for samples 1 and 2, and at $40-120pg$ for sample 3
- Dropout occurred with more frequency beginning at $0.125ng$

Mixture Study

- For all three mixture sets, major-minor contributors were easily distinguishable beginning at the 3:1 and 1:3 ratios
- Mixture profiles were non-concordant 100% samples
- One of the three reasons listed above

Signature Noise Study

- Average background noise for 3, 5, and 10 second injections were 7.6, 8.8, and 11.65 RFU/s, respectively

CONCLUSIONS

- The GeneMapper[®]ID-X v12 software was able to produce accurate, reliable, reproducible and concordant results to those obtained using GeneMapper[®]ID v3.1
- The procedure studies showed that GMD-X can provide precise and concordant results
- The known, NIST, and non-probative samples showed concordance to both published data as well as previously analyzed data using GMD
- For the user defined settings available in GMD-X a minimum peak calling threshold of 50 RFU is recommended for both AB¹ 3100-A and AB² 3100-B
- Any non-concordance found between GMD-X and GMD could be attributed to a cause unrelated to the software program
- Throughout the validation, GMD-X v12 performed as expected
- GMD-X is suitable for use in forensic casework with PowerPlex[®]HS and PFSO[®] AB¹ 3100-A and B instruments
- GMD-X has been validated for use with casework samples and the foundation for its validation for use as an expert system for known single source samples has been established
- Both the mixture tools in GMD-X and ArmaDeQ[™] proved to be effective in aiding in mixture deconvolution

REFERENCES

1. Power, T. B. Mccabe, and D. Harrison. "ATSD DNA: A New Expert System for Forensic DNA Analysis." Forensic Science International: Genetics 2:3 (2008): 193-6.
2. Applied Biosystems. GeneMapper[®]ID-X Software v12 Product Bulletin. Foster City, CA: Applied Biosystems, 2007.
3. Frazier, Roger, Catherine, Lisa, and Lani Schalk. "Is 'Improving Forensic DNA Laboratory Through: Enhanced Data Analysis and Expert System Capabilities' Page 4." Forensic Magazine. Web. 07 Dec. 2011.
4. Roby, Rhonda K. "Using the Future Phase of the NIST Project." Lecture Association of Forensic DNA Analysts and Administrators. Austin, TX, 20 Jan. 2009. Marshall University. Forensic Science NEST. Project Reference Materials. N/A. Web. Mar-Apr. 2011. http://forensics.marshall.edu/NEST/PFSO/NEST/Investigation/ID-X/2009_Roby.pdf
5. Applied Biosystems. GeneMapper[®]ID-X Software Version 12 User Bulletin. Foster City, CA: Applied Biosystems, December 2010.
6. Roby, Rhonda K., and Amy D. Christen. "Validating Expert Systems: Examples with the PFSO Expert System Software." Forensic DNA (September 2007): 13-15.

INTRODUCTION

The discontinuation of the Applied Biosystems' 3100 System Genetic Analyzers, GMD-X's new mixture analysis tool, and the gradual interest in the implementation of expert systems into forensic laboratories, led PFSO to purchase GeneMapper[®]ID-X v12. This validation was intended to test the robustness, reliability and sensitivity of the GMD-X software and its concordance with GMD to demonstrate that it is suitable for use in forensic casework with PowerPlex[®]HS and the PFSO AB¹ 3100-A and AB² 3100-B.

All algorithms in GeneMapper[®]ID-X are unchanged from GeneMapper[®]ID v3.1 (GMD). This, along with similar user interfaces, will allow for a smooth transition for analysts from GMD to GMD-X. Furthermore, with the capability to analyze both the and PFSO sample files GMD-X can act as a long term software system for laboratories looking to maintain current analysis protocols while providing flexibility for future advancements in technology. GMD-X not only allows for the streamlining of data analysis, it also qualifies as an expert system by assisting in the manual review of single source samples.

Both GMD-X and the recently released ArmaDeQ[™] software program from Nicholson Forensics, LLC contain new mixture analysis tools meant to assist analysts in deconvoluting two and three-person mixtures and help provide a laboratory with a common platform from which to interpret DNA mixtures.

REFERENCES

1. Power, T. B. Mccabe, and D. Harrison. "ATSD DNA: A New Expert System for Forensic DNA Analysis." Forensic Science International: Genetics 2:3 (2008): 193-6.
2. Applied Biosystems. GeneMapper[®]ID-X Software v12 Product Bulletin. Foster City, CA: Applied Biosystems, 2007.
3. Frazier, Roger, Catherine, Lisa, and Lani Schalk. "Is 'Improving Forensic DNA Laboratory Through: Enhanced Data Analysis and Expert System Capabilities' Page 4." Forensic Magazine. Web. 07 Dec. 2011.
4. Roby, Rhonda K. "Using the Future Phase of the NIST Project." Lecture Association of Forensic DNA Analysts and Administrators. Austin, TX, 20 Jan. 2009. Marshall University. Forensic Science NEST. Project Reference Materials. N/A. Web. Mar-Apr. 2011. http://forensics.marshall.edu/NEST/PFSO/NEST/Investigation/ID-X/2009_Roby.pdf
5. Applied Biosystems. GeneMapper[®]ID-X Software Version 12 User Bulletin. Foster City, CA: Applied Biosystems, December 2010.
6. Roby, Rhonda K., and Amy D. Christen. "Validating Expert Systems: Examples with the PFSO Expert System Software." Forensic DNA (September 2007): 13-15.

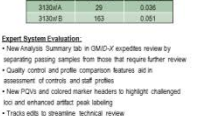


Figure 1: GMD-X Analysis Summary tab



Figure 2: ArmaDeQ[™] Mixture Interpretation Window

MATERIALS AND METHODS

- No files from previously generated data using PowerPlex[®]HS and the 3100s were used for this validation
- During each study allele calls, basepairs, and heights in relative fluorescent units (RFU) for each sample generated by GMD-X were compared to the results given by GMD
- The studies conducted were as follows: (1) Known Samples and Stratter; (2) NIST Samples/Concordance; (3) Reproducibility; (4) Non-Probative Casework Samples; (5) Precision; (6) Signal to Noise; (7) Sensitivity and Analytical Threshold Studies and (8) Mixture Studies

ACKNOWLEDGMENTS

I thank Dr. Head Honcho, Palm Beach County Sheriff's Office Forensic Biology Unit (PFSO) Laboratory Supervisor, Colleague B, FSU Technical Liaison, Colleague C, FSU Senior Forensic Scientist, and Colleague A, FSU Forensic Scientist, for all of their assistance and support during this project. I also thank Analyst A and Analyst B of the Marshall University Forensic Science DNA Laboratory and Dr. Rippen Dawn Marshall University top advisor for their help and support. A large thank you goes out to Nicholson Forensic LLC. This project was supported by Award No. 2008-DN-BA-421 awarded by the National Institute of Justice, Office of Justice Programs, U.S. Department of Justice. The opinions, findings and conclusions expressed in this paper are those of the author(s) and do not reflect the views of the Department of Justice.



Figure 1: GMD-X Analysis Summary tab



Figure 2: ArmaDeQ[™] Mixture Interpretation Window



Internal Validation of GeneMapper[®]ID-X for use in Forensic Casework

Former Student, BS¹; Colleague A, MFS²; Colleague B, MS³; Colleague C, MS⁴; Head Honcho, PhD⁵
¹Marshall University, Forensic Science Department, 1401 Forensic Science Dr., Huntington, WV 25701
²Palm Beach County Sheriff's Office, Forensic Biology Unit, 3228 Gun Club Rd., West Palm Beach, FL 33406



ABSTRACT

Due to the implementation of robotic equipment to extract, quantify, amplify, and detect forensic DNA samples, the bottleneck of forensic DNA analysis has shifted to data interpretation. There is now a need for computer software that maximizes efficiency and minimizes the resources needed for DNA analysis. Applied Biosystems' GeneMapper[®]ID-X is one of the software systems capable of reducing this bottleneck and providing a suite of tools to assist in single source and DNA mixture interpretation. GeneMapper[®]ID-X v12 (GMD-X) was validated for use with questioned casework samples and a foundation to utilize the expert system capabilities for known casework samples was established. Original GeneMapper[®]ID v3.1 (GMD) validation data was analyzed with GMD-X and the results were compared. The GMD-X software was able to produce accurate, reliable, reproducible and concordant results to those obtained using GMD. It was also the goal of this project to find a software system that can aid in performing interpretation of DNA mixtures. Therefore, the mixture deconvolution tool portions of both GMD-X and Nicholson Forensics, LLC's ArmaDeQ[™] were evaluated for their use in deconvoluting two and three-person DNA mixtures.

RESULTS AND DISCUSSION

Known Samples and Stratter Studies

- Known samples were concordant for 29/31 known samples compared to the data analyzed using GMD
- The first non-concordance could be attributed to a lower calling threshold, while the second was due to a failure in Size Quality
- Generally, the recommended stutter %s for PFSO with GMD-X were less than those published by PowerGen

Sensitivity and Analytical Threshold Studies

- 3100-A PFR kit below 10% with greater frequency at $40-120pg$ for all three reagent times and at three sample sets
- 3100-B PFR kit below 10% with greater frequency at $40-120pg$ for samples 1 and 2, and at $40-120pg$ for sample 3
- Dropout occurred with more frequency beginning at $0.125ng$

Mixture Study

- For all three mixture sets, major-minor contributors were easily distinguishable beginning at the 3:1 and 1:3 ratios
- Mixture profiles were non-concordant 100% samples
- One of the three reasons listed above

Signature Noise Study

- Average background noise for 3, 5, and 10 second injections were 7.6, 8.8, and 11.65 RFU/s, respectively

CONCLUSIONS

- The GeneMapper[®]ID-X v12 software was able to produce accurate, reliable, reproducible and concordant results to those obtained using GeneMapper[®]ID v3.1
- The procedure studies showed that GMD-X can provide precise and concordant results
- The known, NIST, and non-probative samples showed concordance to both published data as well as previously analyzed data using GMD
- For the user defined settings available in GMD-X a minimum peak calling threshold of 50 RFU is recommended for both AB¹ 3100-A and AB² 3100-B
- Any non-concordance found between GMD-X and GMD could be attributed to a cause unrelated to the software program
- Throughout the validation, GMD-X v12 performed as expected
- GMD-X is suitable for use in forensic casework with PowerPlex[®]HS and PFSO[®] AB¹ 3100-A and B instruments
- GMD-X has been validated for use with casework samples and the foundation for its validation for use as an expert system for known single source samples has been established
- Both the mixture tools in GMD-X and ArmaDeQ[™] proved to be effective in aiding in mixture deconvolution

REFERENCES

1. Power, T. B. Mccabe, and D. Harrison. "ATSD DNA: A New Expert System for Forensic DNA Analysis." Forensic Science International: Genetics 2:3 (2008): 193-6.
2. Applied Biosystems. GeneMapper[®]ID-X Software v12 Product Bulletin. Foster City, CA: Applied Biosystems, 2007.
3. Frazier, Roger, Catherine, Lisa, and Lani Schalk. "Is 'Improving Forensic DNA Laboratory Through: Enhanced Data Analysis and Expert System Capabilities' Page 4." Forensic Magazine. Web. 07 Dec. 2011.
4. Roby, Rhonda K. "Using the Future Phase of the NIST Project." Lecture Association of Forensic DNA Analysts and Administrators. Austin, TX, 20 Jan. 2009. Marshall University. Forensic Science NEST. Project Reference Materials. N/A. Web. Mar-Apr. 2011. http://forensics.marshall.edu/NEST/PFSO/NEST/Investigation/ID-X/2009_Roby.pdf
5. Applied Biosystems. GeneMapper[®]ID-X Software Version 12 User Bulletin. Foster City, CA: Applied Biosystems, December 2010.
6. Roby, Rhonda K., and Amy D. Christen. "Validating Expert Systems: Examples with the PFSO Expert System Software." Forensic DNA (September 2007): 13-15.

INTRODUCTION

The discontinuation of the Applied Biosystems' 3100 System Genetic Analyzers, GMD-X's new mixture analysis tool, and the gradual interest in the implementation of expert systems into forensic laboratories, led PFSO to purchase GeneMapper[®]ID-X v12. This validation was intended to test the robustness, reliability and sensitivity of the GMD-X software and its concordance with GMD to demonstrate that it is suitable for use in forensic casework with PowerPlex[®]HS and the PFSO AB¹ 3100-A and AB² 3100-B.

All algorithms in GeneMapper[®]ID-X are unchanged from GeneMapper[®]ID v3.1 (GMD). This, along with similar user interfaces, will allow for a smooth transition for analysts from GMD to GMD-X. Furthermore, with the capability to analyze both the and PFSO sample files GMD-X can act as a long term software system for laboratories looking to maintain current analysis protocols while providing flexibility for future advancements in technology. GMD-X not only allows for the streamlining of data analysis, it also qualifies as an expert system by assisting in the manual review of single source samples.

Both GMD-X and the recently released ArmaDeQ[™] software program from Nicholson Forensics, LLC contain new mixture analysis tools meant to assist analysts in deconvoluting two and three-person mixtures and help provide a laboratory with a common platform from which to interpret DNA mixtures.

RESULTS AND DISCUSSION

Known Samples and Stratter Studies

- Known samples were concordant for 29/31 known samples compared to the data analyzed using GMD
- The first non-concordance could be attributed to a lower calling threshold, while the second was due to a failure in Size Quality
- Generally, the recommended stutter %s for PFSO with GMD-X were less than those published by PowerGen

Sensitivity and Analytical Threshold Studies

- 3100-A PFR kit below 10% with greater frequency at $40-120pg$ for all three reagent times and at three sample sets
- 3100-B PFR kit below 10% with greater frequency at $40-120pg$ for samples 1 and 2, and at $40-120pg$ for sample 3
- Dropout occurred with more frequency beginning at $0.125ng$

Mixture Study

- For all three mixture sets, major-minor contributors were easily distinguishable beginning at the 3:1 and 1:3 ratios
- Mixture profiles were non-concordant 100% samples
- One of the three reasons listed above

Signature Noise Study

- Average background noise for 3, 5, and 10 second injections were 7.6, 8.8, and 11.65 RFU/s, respectively

CONCLUSIONS

- The GeneMapper[®]ID-X v12 software was able to produce accurate, reliable, reproducible and concordant results to those obtained using GeneMapper[®]ID v3.1
- The procedure studies showed that GMD-X can provide precise and concordant results
- The known, NIST, and non-probative samples showed concordance to both published data as well as previously analyzed data using GMD
- For the user defined settings available in GMD-X a minimum peak calling threshold of 50 RFU is recommended for both AB¹ 3100-A and AB² 3100-B
- Any non-concordance found between GMD-X and GMD could be attributed to a cause unrelated to the software program
- Throughout the validation, GMD-X v12 performed as expected
- GMD-X is suitable for use in forensic casework with PowerPlex[®]HS and PFSO[®] AB¹ 3100-A and B instruments
- GMD-X has been validated for use with casework samples and the foundation for its validation for use as an expert system for known single source samples has been established
- Both the mixture tools in GMD-X and ArmaDeQ[™] proved to be effective in aiding in mixture deconvolution

REFERENCES

1. Power, T. B. Mccabe, and D. Harrison. "ATSD DNA: A New Expert System for Forensic DNA Analysis." Forensic Science International: Genetics 2:3 (2008): 193-6.
2. Applied Biosystems. GeneMapper[®]ID-X Software v12 Product Bulletin. Foster City, CA: Applied Biosystems, 2007.
3. Frazier, Roger, Catherine, Lisa, and Lani Schalk. "Is 'Improving Forensic DNA Laboratory Through: Enhanced Data Analysis and Expert System Capabilities' Page 4." Forensic Magazine. Web. 07 Dec. 2011.
4. Roby, Rhonda K. "Using the Future Phase of the NIST Project." Lecture Association of Forensic DNA Analysts and Administrators. Austin, TX, 20 Jan. 2009. Marshall University. Forensic Science NEST. Project Reference Materials. N/A. Web. Mar-Apr. 2011. http://forensics.marshall.edu/NEST/PFSO/NEST/Investigation/ID-X/2009_Roby.pdf
5. Applied Biosystems. GeneMapper[®]ID-X Software Version 12 User Bulletin. Foster City, CA: Applied Biosystems, December 2010.
6. Roby, Rhonda K., and Amy D. Christen. "Validating Expert Systems: Examples with the PFSO Expert System Software." Forensic DNA (September 2007): 13-15.

MATERIALS AND METHODS

- No files from previously generated data using PowerPlex[®]HS and the 3100s were used for this validation
- During each study allele calls, basepairs, and heights in relative fluorescent units (RFU) for each sample generated by GMD-X were compared to the results given by GMD
- The studies conducted were as follows: (1) Known Samples and Stratter; (2) NIST Samples/Concordance; (3) Reproducibility; (4) Non-Probative Casework Samples; (5) Precision; (6) Signal to Noise; (7) Sensitivity and Analytical Threshold Studies and (8) Mixture Studies

ACKNOWLEDGMENTS

I thank Dr. Head Honcho, Palm Beach County Sheriff's Office Forensic Biology Unit (PFSO) Laboratory Supervisor, Colleague B, FSU Technical Liaison, Colleague C, FSU Senior Forensic Scientist, and Colleague A, FSU Forensic Scientist, for all of their assistance and support during this project. I also thank Analyst A and Analyst B of the Marshall University Forensic Science DNA Laboratory and Dr. Rippen Dawn Marshall University top advisor for their help and support. A large thank you goes out to Nicholson Forensic LLC. This project was supported by Award No. 2008-DN-BA-421 awarded by the National Institute of Justice, Office of Justice Programs, U.S. Department of Justice. The opinions, findings and conclusions expressed in this paper are those of the author(s) and do not reflect the views of the Department of Justice.



Figure 1: GMD-X Analysis Summary tab



Figure 2: ArmaDeQ[™] Mixture Interpretation Window

Size: 48" x 36"

Size: 50" x 36"

Images (cont.)

- ▣ Always acknowledge your sources
- ▣ Images must already exist
 - beware of copyright issues
 - can be resized, rotated
 - high quality images
 - beware of screen captures
 - ▣ spelling mistakes (or big, scientific words) can not be changed

Spelling mistakes can't be changed when you copy/paste a screen capture

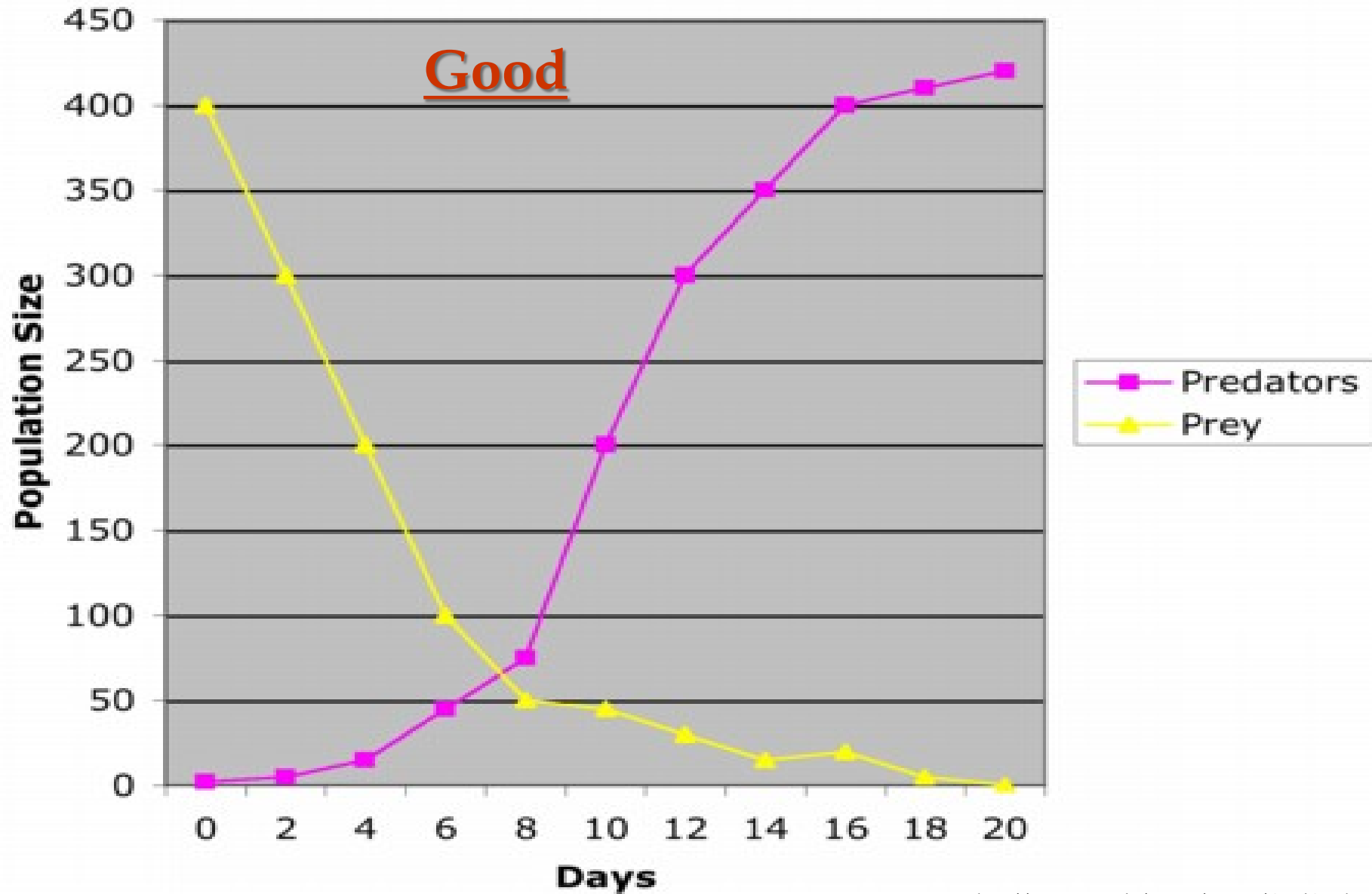
Candidate Gene Abbreviation and Name	SNP Frequency
AGT (<u>angiotensinogen preprotein</u>)	2
APOA (<u>apolipoprotein A1, A4, and A5</u>)	3
APOB (<u>apolipoprotein B</u>)	7
APOC2 (<u>apolipoprotein C-II</u>)	2
APOE (<u>apolipoprotein E</u>)	1
BHMT (<u>betaine-homocysteine methyltransferase</u>)	3
CBS (<u>cystathionine beta-synthase</u>)	3
CETP (<u>cholesteryl ester transfer protein</u>)	17
CRP (<u>c-reactive protein</u>)	1
F5 (<u>coagulation factor V</u>)	1
FOLH (<u>folate hydrolase</u>)	1
HDLBP (<u>high density lipoprotein binding protein</u>)	1
HNF4A (<u>hepatocyte nuclear factor 4, alpha</u>)	2
LCAT (<u>lecithin: cholesterol acyltransferase</u>)	1
LDLR (<u>low density lipoprotein receptor</u>)	1
LIPC (<u>lipase, hepatic</u>)	2
LIPG (<u>lipase, endothelial</u>)	1
LPL (<u>lipoprotein lipase</u>)	2
LRP1 (<u>low density lipoprotein-related protein 1</u>)	2
LRP1B (<u>low density lipoprotein-related protein 1B</u>)	7
LRP5 (<u>low density lipoprotein receptor-related protein 5</u>)	7
LPR8 (<u>low density lipoprotein receptor-related protein 8</u>)	4
MPO (<u>myeloperoxidase</u>)	2
MSR1 (<u>macrophage scavenger receptor 1</u>)	1
MTR (<u>5-methyltetrahydrofolate-homocysteine</u>)	1
MTRR (<u>methionine synthase reductase</u>)	1
NOS3 (<u>nitric oxide synthase 3</u>)	3
PLTP (<u>phospholipid transfer protein</u>)	2
PON (<u>paroxonase</u>)	8
PPARA (<u>peroxisome proliferative activated receptor</u>)	7
Total: 30	96

It will print exactly as it shows up...
red squiggly lines included

Graphs

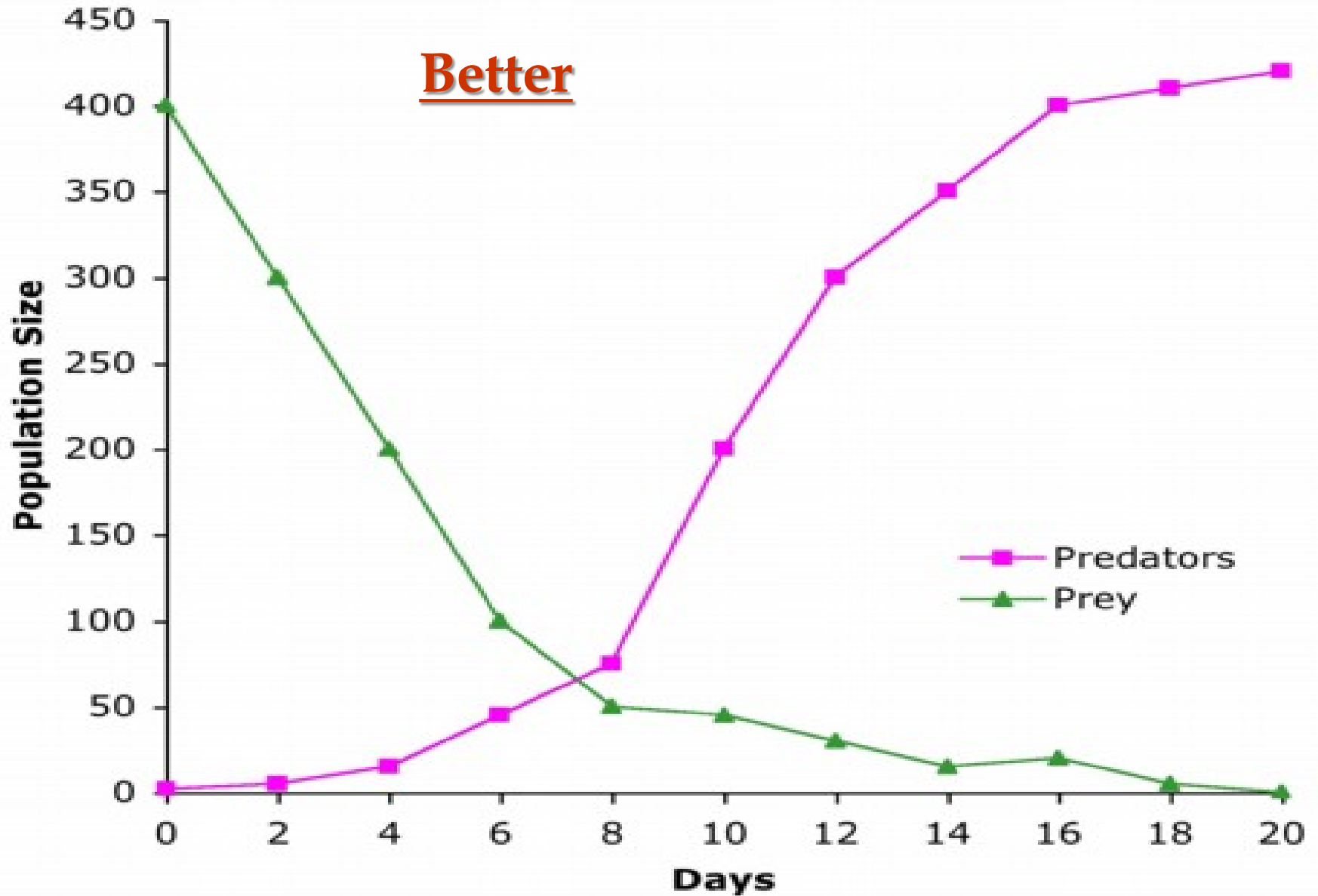
- ▣ Focus on your data
 - keep graphs clean and simple
- ▣ Being exact and specific has its place
 - but it's better to get the message across
- ▣ No distractions
 - your message will come through loud and clear

Population Sizes Through Time



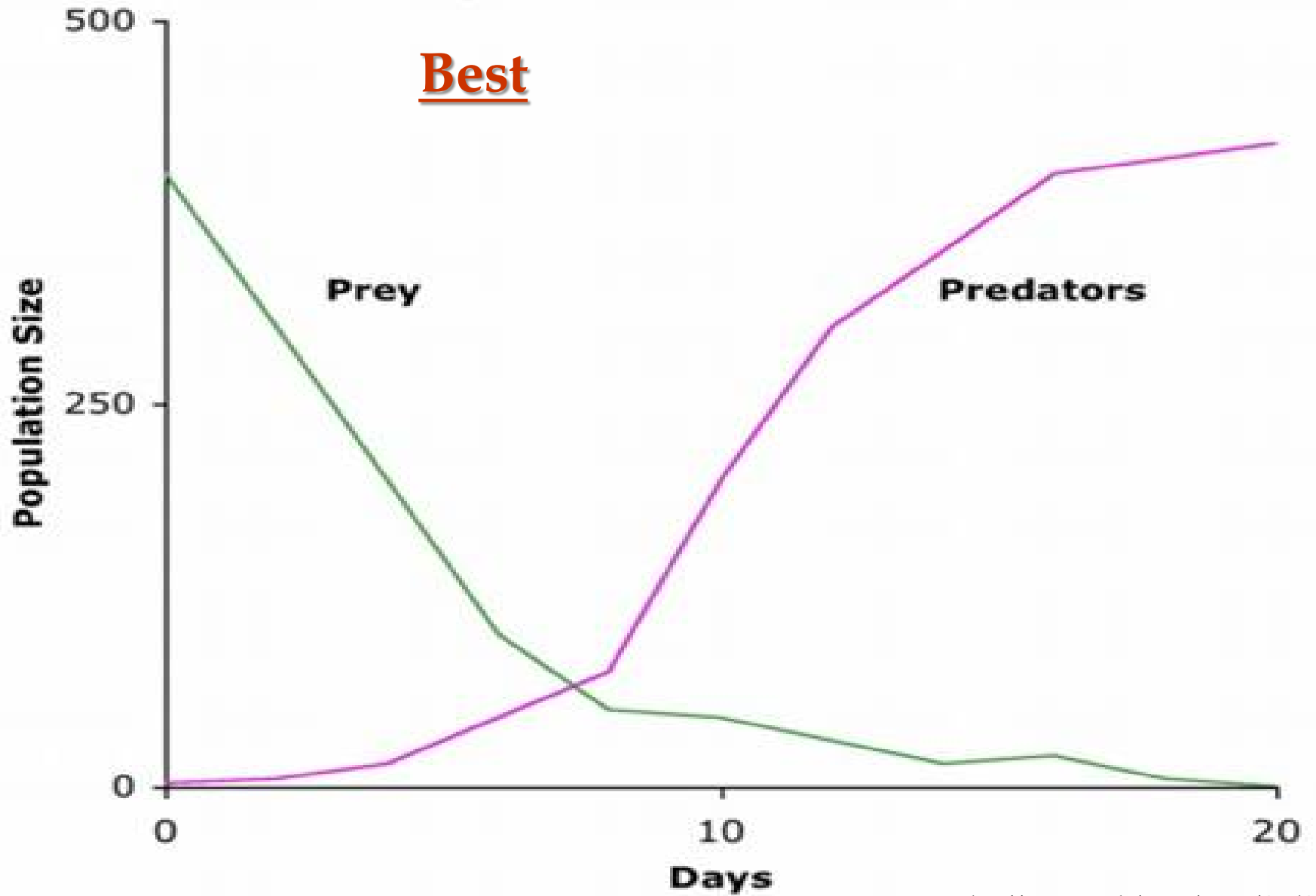
Population Sizes Through Time

Better



Population Sizes Through Time

Best



Composition

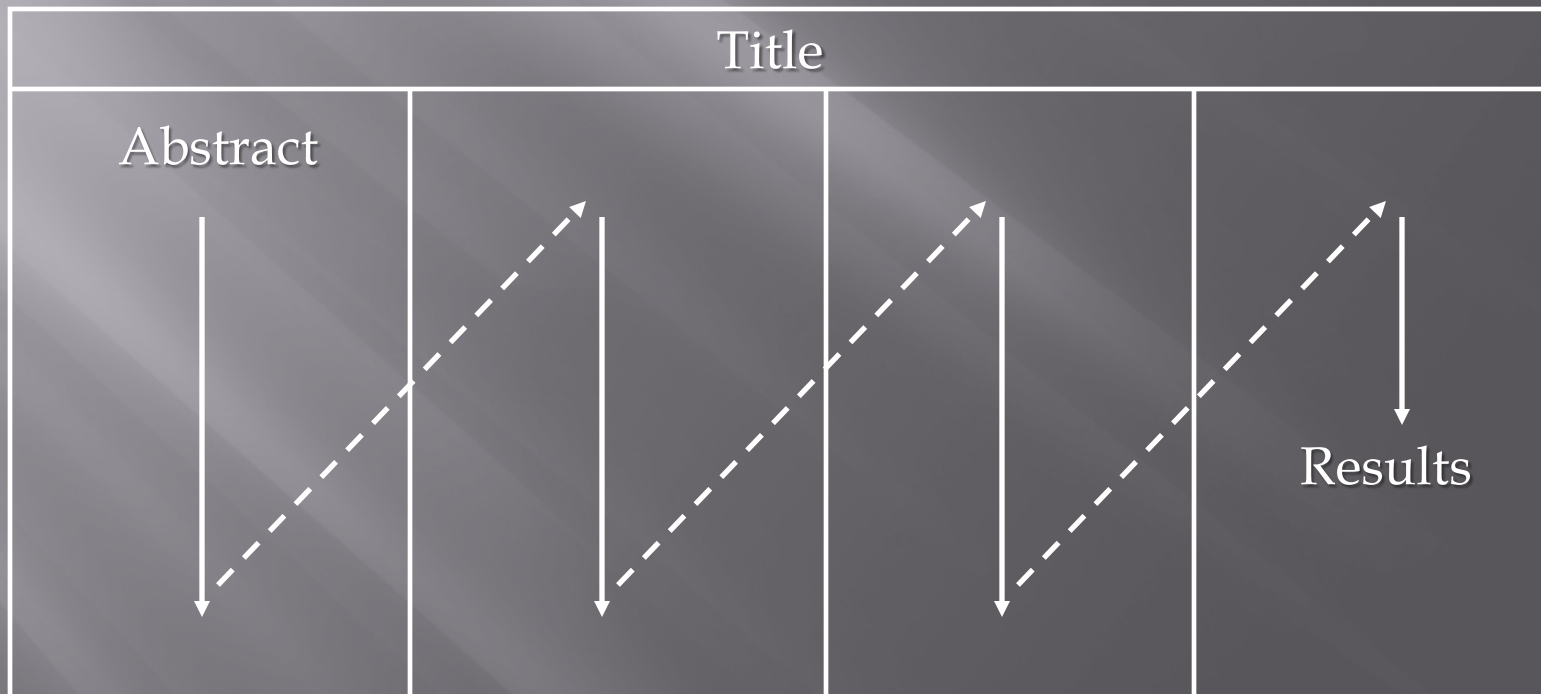
- ▣ Font size is font size
 - 20 pt TNR is 20 pt TNR
 - don't be fooled by apparent size
 - ▣ on monitor
 - ▣ test print on desktop printer

Composition (cont.)

- ▣ Calibri is better for computer monitor
 - Powerpoint default
- ▣ TNR is better for paper, therefore poster
 - Titles: 80 – 96 pt
 - Authors: 54 – 60 pt; Address: 40 – 48 pt
 - Section headings: 36 – 40 pt
 - Text, References: 28 – 32 pt
 - Acknowledgments: 18 – 24 pt

Composition (cont.)

- ▣ Sketch your layout before you start



Backgrounds

- ▣ Do:
 - use native PPT background
 - keep backgrounds simple
 - ▣ solid color or gentle graphic

- ▣ Do not:
 - use backgrounds that fade from light/dark
 - ▣ very distracting
 - use a photo
 - ▣ often creates unpredictable results



Weight Loss Outcomes With High Protein, Low Carbohydrate, Unlimited Calorie Diet

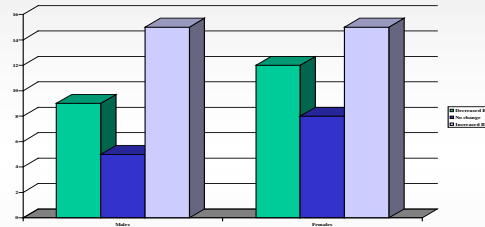
Department of Pediatrics, Joan C. Edwards School of Medicine, Huntington, West Virginia

Introduction: Childhood obesity is currently a national epidemic. The prevalence of childhood overweight (BMI>85%) and obesity (BMI>95%) has doubled in the last 20 years. Traditional interventions with a low fat diet and exercise have been unsuccessful for weight reduction.

Objective: The purpose of our study was to determine the change in BMI in overweight children referred to the endocrine clinic managed with a high protein, low carbohydrate, unlimited calorie diet for six months.

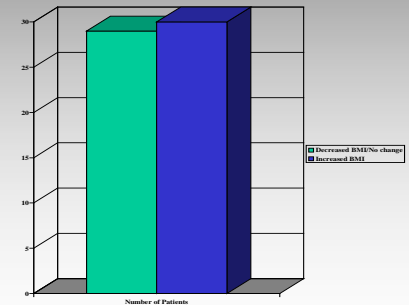
Methods: A retrospective chart review was conducted of all patients referred to the pediatric endocrine clinic over a six year time period with the diagnosis of overweight and obesity. Initial dates of visit, height, and weight were recorded from each patient and on follow up visit six months later. Each patient was counseled on a high protein, low carbohydrate, unlimited calorie diet. BMI was calculated for the initial visit and the follow up visits. Patients with a diagnosis of diabetes mellitus or in which accurate weight could not be assessed were excluded.

Results: A total of 59 patients aged 6-18 years participated in the study. Patients were included in the study if follow up data was available 6 months after the initial visit. 20 (36%) of 59 patients had a decrease in BMI at the follow up visit. 8 (13%) patients had no change in BMI and 30 (51%) patients had an increase in their BMI. Average BMI decrease in those patients with weight loss was 2.76 points (SD 4.85). Average weight loss in the 21 patients with a drop in BMI was 10.3 pounds (SD 13.5).



Discussion: The prevalence of overweight and obesity is increasing in the US. The prevalence of obesity has doubled in the past 20 years. Currently, about 15 % of children ages 6-19 are obese. This trend is seen in the US and other developed countries. Increased rates of obesity are also seen in minorities and disadvantaged children. Body mass index (BMI), the ratio of the weight in kilograms to the square of the height in meters, correlates well with body fatness and other obesity related conditions. Our study aimed to measure the weight loss and decrease in BMI in patients on a high protein, low carbohydrate, and unlimited calorie diet. Their primary care physicians referred patients for obesity. A retrospective chart review was done on over 200 chart of patients referred to the clinic. Follow-up data was available on 59 patients. More than one-third of patients decreased their BMI in this study. The average BMI decrease was 2.76 points (SD 4.85) and 10.3 pounds (SD13.5 pounds). This data is in comparison to the very poor success rates in traditional low calorie, low fat diets. In conjunction with exercise, patients on the high protein, low carbohydrate, unlimited calorie diet can successfully lose weight. Pediatric patients can then use this weight loss as a stepping-stone to a healthier more active lifestyle that includes better food choices for the long term.

Not Good



Conclusion: We have demonstrated a high protein, low carbohydrate, unlimited calorie diet is effective in maintaining or reducing BMI and weight over a six month time period in 49% of overweight children. This approach has been more effective than the traditional low calorie diet with exercise at our institution.



Weight Loss Outcomes With High Protein, Low Carbohydrate, Unlimited Calorie Diet

Department of Pediatrics, Joan C. Edwards School of Medicine, Huntington, West Virginia

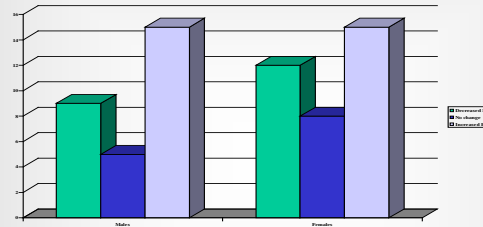
Not Good

Introduction: Childhood obesity is currently a national epidemic. The prevalence of childhood overweight (BMI>85%) and obesity (BMI>95%) has doubled in the last 20 years. Traditional interventions with a low fat diet and exercise have been unsuccessful for weight reduction.

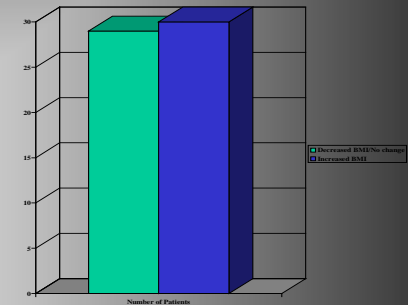
Objective: The purpose of our study was to determine the change in BMI in overweight children referred to the endocrine clinic managed with a high protein, low carbohydrate, unlimited calorie diet for six months.

Methods: A retrospective chart review was conducted of all patients referred to the pediatric endocrine clinic over a six year time period with the diagnosis of overweight and obesity. Initial dates of visit, height, and weight were recorded from each patient and on follow up visit six months later. Each patient was counseled on a high protein, low carbohydrate, unlimited calorie diet. BMI was calculated for the initial visit and the follow up visits. Patients with a diagnosis of diabetes mellitus or in which accurate weight could not be assessed were excluded.

Results: A total of 59 patients aged 6-18 years participated in the study. Patients were included in the study if follow up data was available 6 months after the initial visit. 20 (36%) of 59 patients had a decrease in BMI at the follow up visit. 8 (13%) patients had no change in BMI and 30 (51%) patients had an increase in their BMI. Average BMI decrease in those patients with weight loss was 2.76 points (SD 4.85). Average weight loss in the 21 patients with a drop in BMI was 10.3 pounds (SD 13.5).



Discussion: The prevalence of overweight and obesity is increasing in the US. The prevalence of obesity has doubled in the past 20 years. Currently, about 15 % of children ages 6-19 are obese. This trend is seen in the US and other developed countries. Increased rates of obesity are also seen in minorities and disadvantaged children. Body mass index (BMI), the ratio of the weight in kilograms to the square of the height in meters, correlates well with body fatness and other obesity related conditions. Our study aimed to measure the weight loss and decrease in BMI in patients on a high protein, low carbohydrate, and unlimited calorie diet. Their primary care physicians referred patients for obesity. A retrospective chart review was done on over 200 chart of patients referred to the clinic. Follow-up data was available on 59 patients. More than one-third of patients decreased their BMI in this study. The average BMI decrease was 2.76 points (SD 4.85) and 10.3 pounds (SD13.5 pounds). This data is in comparison to the very poor success rates in traditional low calorie, low fat diets. In conjunction with exercise, patients on the high protein, low carbohydrate, unlimited calorie diet can successfully lose weight. Pediatric patients can then use this weight loss as a stepping-stone to a healthier more active lifestyle that includes better food choices for the long term.



Conclusion: We have demonstrated a high protein, low carbohydrate, unlimited calorie diet is effective in maintaining or reducing BMI and weight over a six month time period in 49% of overweight children. This approach has been more effective than the traditional low calorie diet with exercise at our institution.



Chmp1, a Strabismus binding protein, plays multiple roles in vertebrate convergent extension movements and tumor formation



¹Biochemistry and Microbiology Dept., School of Medicine, Marshall University, Huntington, WV,

²Pharmacology Dept., HHMI, University of Washington, Seattle WA, ³Zoology Dept., University of Washington, Seattle WA

Not Good

ABSTRACT

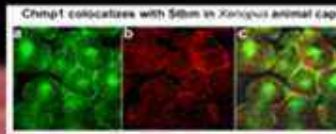
Strabismus (*Strab*) mediates convergent extension movements during gastrulation in vertebrates as a component of the Planar Cell Polarity (PCP) pathway. Chromatin modifying protein 1 (Chmp1) was identified as a *Strab* binding protein by using a yeast two-hybrid screen. Chmp1 protein is highly conserved through out evolution and belongs to a family of nucleosome tracking proteins (Charged Multivesicular Body Protein). However, the function of Chmp1 in vertebrate development as well as its signaling activities have barely been investigated.

We have confirmed the interaction between *Strab* and Chmp1 and have shown the co-localization of *Strab* and Chmp1. We also demonstrated that functionally Chmp1 regulated convergent extension movements in zebrafish similar to *Strab*. Chmp1 function in gastrulation movements appears to be the consequence of the activation of AP-1 complex via PCP pathway.

In addition, we have shown that Chmp1 induced hyperplasia in zebrafish when its function was over-regulated. In NIH 3T3 cells, exogenous Chmp1 induced the inhibition of cell growth. Subsequently, NIH 3T3 cells were transfected to grow anchorage-independent when Chmp1 was knocked down by siRNA. The data from NIH 3T3 cells indicates that Chmp1 may function as a tumor suppressor. We established the potential tumor suppressor function of Chmp1 by screening human cancer profiling arrays and human tumor tissue arrays. Chmp1 mRNA was specifically reduced in various pancreatic tumor samples compared to corresponding normal samples. Indeed, Chmp1 protein was absent in the cancer cells of pancreatic tumors.



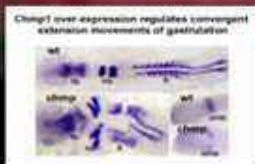
As seen in the wild type, Chmp1 associates with Strab in which heteroimmunoprecipitation (IP) with HA-tagged Chmp1 and Western Blotting for Myc-tagged Strab. First lane is a Strab input and second lane is a control.



GFP-tagged Chmp1 protein (green) is localized to the cytoplasm, nucleus, and membrane (A). Endogenous Strab protein (red) is localized at the membrane (B). Chmp1 co-localizes with Strab at the membrane (yellow) as can be seen in C.



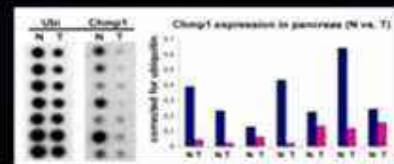
Chmp1 siRNA knock-down Chmp1 protein and β -actin is used as a loading control (A). NIH 3T3 cells are transfected to form colonies (arrows) in soft agar when Chmp1 is knocked-down by siRNA (B). Control siRNA delivered NIH 3T3 cells do not form colonies.



Fluorescent zebrafish embryos, wild type (WT) and Chmp1 over-expressing (over) embryos, headless and tailless are visualized with DAPI, Krc2-3, and MyoD respectively. Chmp1 over-expression at embryo has a shorter and wider body axis with open neural tube (C).



Shown at 41 and 42 as the same embryo, light and fluorescent (GFP) immunofluorescence microscopy. GFP tagged Chmp1 is expressed in the dorsal part of the embryo (arrows) at the dorsal side of the embryo increases as the embryo grows older, shown in arrows (B) in the same embryo in B1, a day after.



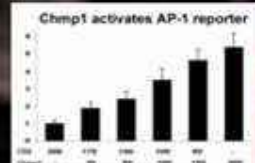
Chmp1 mRNA is strongly reduced in pancreatic tumors. Clontech Cancer Profiling Assay II hybridized with human ubiquitin (*Ub*, control) and Chmp1 cDNA probes demonstrates the reduction of Chmp1 mRNA in various pancreatic tumors. Densitometric analysis of array exhibits 1.5 to 30 fold reduction of Chmp1 mRNA in pancreatic tumors.

INTRODUCTION

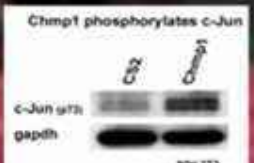
Previously we have reported that Strabismus (*Strab*), a component of PCP (Planar Cell Polarity) pathway, regulates convergent extension movements in vertebrates. We demonstrated that *Strab* inherited its gastrulation movements by gain of and loss of functional copy. Mechanistically, *Strab* was shown to inhibit *Chordin* mediated Wnt signaling activity. In addition, *Strab* activated *c-Jun* mediated AP-1 reporter and phosphorylated *c-Jun*. Based on the data, we hypothesized the *Strab*, by its binding with *Dax*, activates *c-Jun* signaling pathway to regulate convergent extension movements.

Using a yeast two-hybrid approach, we identified Chmp1 (Chromatin Modifying Protein 1/Charged Multivesicular Body Protein) as a *Strab* associated protein. Chmp1 was reported to silence gene activation by interacting with transcriptional repressor Polycomb group (PcG) protein, Polycomb-like (Pol). Over-expression studies demonstrated that the gene silencing of Chmp1 was due to its effect on the chromatin structure and cell cycle progression. Chmp1 was also shown to physically associate with multivesicular body protein, SKD1/VP4 (vesicular protein-4). We identified a homolog of Chmp1 named SAL1 (supernumerary allelic layer 1) was also identified. SAL1 was shown to be involved in regulating the formation of a tubular cell layer in maize grain. Mutation in *sal1* results in more aleurone cell layers suggesting that SAL1 might play a role in growth. Taken together, these studies indicate that Chmp1 may play a role in vertebrate development by controlling cell growth and receptor activity.

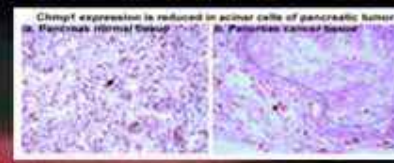
We cloned Chmp1 from zebrafish as a *Strab* associated protein using a yeast two-hybrid screen. Similar to *Strab*, Chmp1 regulated convergent extension movements of gastrulation by activating AP-1 complex, a downstream target of the PCP pathway. Additionally, Marshall's media led Chmp1 knockdown induced abnormal cell growth in zebrafish. In addition, Chmp1 knockdown by siRNA rendered NIH 3T3 cells to grow in an anchorage independent manner. The siRNA knockdown assays indicated that Chmp1 might function in human tumor development. To test this hypothesis, we measured Chmp1 mRNA and protein level in cancer tissue samples and compared with the level in corresponding normal tissues. Chmp1 mRNA was strongly reduced in various pancreatic tumor tissues when compared with corresponding normal tissues. Furthermore, Chmp1 protein was nearly absent from the cancer cells of pancreatic tumor tissues. Taken together, our study indicates that Chmp1 function in convergent extension movements and tumor development in vertebrates.



Luciferase reporter assay showing Chmp1 plants activates AP-1 in a dose dependent manner in NIH 3T3 cells.



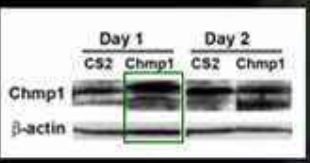
Chmp1 phosphorylates c-Jun at Serine 73 in NIH 3T3 cells. C62 vector is transfected as a control. The level of gapdh is blotted to verify protein loading.



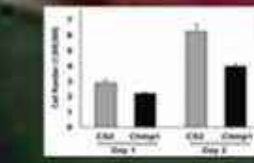
Chmp1 protein is absent absent from the cancer cells of pancreatic tumor. Chmp1 protein is localized to the surface of the normal cells of pancreas (arrows). In tumor, Chmp1 protein expression is almost absent from the cancer cells (control area) even though its expression is unaffected in the rest of the tissue (C).

Conclusions

- Chmp1 binds and co-localizes with Strab.
- Chmp1 regulates convergent extension movements.
- Chmp1 misregulation induces hyperplasia in zebrafish.
- Chmp1 over-expression inhibits growth in NIH 3T3 cells.
- Chmp1 knockdown results in anchorage-independent colony formation.
- Chmp1 mRNA and protein expression is highly reduced in pancreatic tumors.



Chmp1 over-expression upon transfection is shown in NIH 3T3 cells (green box). C62 vector is transfected as a control. β -actin is used as a loading control.



Chmp1 over-expression induces growth inhibition in NIH 3T3 cells. An assay was taken from three separate experiments.

This Research has been supported in part by NIH COBRE (Center for Biomedical Research Excellence, RR02193-02) and WV Blue Printer Science and Technology Research Challenge Fund (EP15-MU-RC-1).

Backgrounds (cont.)

- ▣ Avoid:
 - burst images
 - strongly mottled images
 - wild colors
- ▣ Remember: simple can be striking!

Not Good



Nitric Oxide and Diet-Induced Hypertension in the Obese Zucker Rat

Abstract

We have shown that obese Zucker rats on a high fat diet develop hypertension when saline is added to their drinking water whereas lean Zucker rats do not. The objective of this study was to determine whether the production of nitric oxide (NO), a potent vasodilator involved in blood pressure regulation is affected by similar dietary manipulation. Eight-week-old female lean and obese Zucker rats were fed a diet high in fat content or standard rat chow (control diet) for 10 weeks. From week 4 through week 10, 1% NaCl was added to their drinking water. Urinary excretion of NO metabolites (NO2 and NO3) was measured at weekly intervals. The excretion of NO metabolites was dramatically reduced within a week of placing the rats on a high fat diet and continued to decline over time, suggesting that the high fat diet may be suppressing NO production. We conclude that the suppression of NO production may be a factor limiting the ability of the obese rat to maintain its blood pressure when challenged with a salt load.

Introduction

Obesity is a well-known risk factor for a wide variety of diseases including hypertension, type II diabetes, and coronary heart disease (Brunner 1999). Consequently, the medical importance of this condition has rapidly escalated in tandem with its prevalence in developed countries throughout the world (World Health Organization 2000).

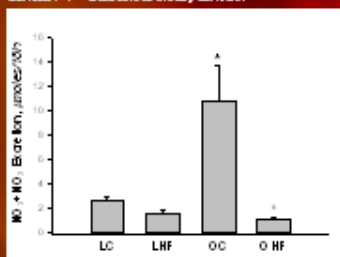
High dietary fat intake has also been independently associated with hypertension and other pathological conditions; however, the link between high fat diets and hypertension has received much less attention than the relation between obesity and hypertension. This disparity is due in part to a very close and confounding relationship between high fat diets and weight gain, which makes it difficult to isolate the direct hypertensive effect of a high fat diet from indirect effects that are mediated through the metabolic alterations of obesity per se. Moreover, high fat diets have been shown to induce insulin resistance independent of obesity in studies of metabolic syndrome X (Barnard 1999, Vesely 2003). Moreover, results of the DASH trials have indicated that low fat diets reduce blood pressure regardless of body weight, although the effects are more pronounced when accompanied by weight loss (Bacon 2006).

One objective of the current study was to determine whether a high fat diet directly promotes the development of hypertension in obese rats. This was done by assessing the effect of a high fat diet on the blood pressure of lean and obese rats before and after they were subjected to an increased salt load. Because NO plays an important role in blood pressure homeostasis, changes in NO production by the different experimental groups were assessed to determine whether alterations in NO production could be involved in the mechanism leading to blood pressure changes induced by the experimental design.

Table 1. Gram percentage of macronutrient components for the control and high fat diets

Diet	Control	High Fat
Protein	23.4	18.5
Carbohydrate	48.1	56.7
Fat	4.5	15.6

Figure 1. NO metabolite excretion in lean control (LC), lean high fat (LHF), obese control (OC), and obese high fat (OHF) experimental groups over 10 weeks. n=9 for lean groups and n=8 for obese groups. *P < 0.05 versus phenotypic controls. +P < 0.05 versus dietary controls.



Departments of ^aPhysiology and ^dCardiovascular Services, Joan C. Edwards School of Medicine at Marshall University, ^bWheeling Jesuit University, ^cWest Liberty State College

Figure 2. Blood pressures of obese (O) and lean (L) Zucker rats on either a high fat or control diet. The arrow just after week 0 indicates when the high fat diet was initiated in high fat groups. The arrow after week 4 indicates when all groups began drinking 1% saline. n=16 for obese groups and n=18 for lean groups. *P < 0.05 versus same week dietary controls.

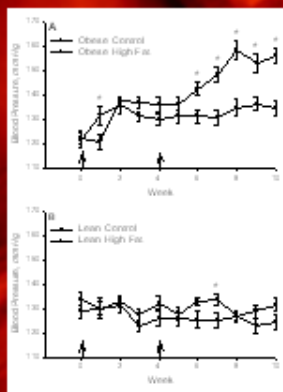
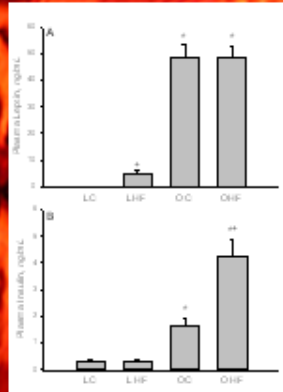


Table 2. Metabolic and cardiovascular characteristics of lean and obese Zucker rats fed a high fat or regular diet. For each lean and obese group, n=9 and n=8, respectively. Values are given in means ± SE. Lee's index of obesity is the cube root of body weight (g) divided by nasoanal length (cm). B (metabolic cumulative energy intake) (CEI), changes in body weight, and energy efficiency ratio (EER) express productivity towards weight gain. Measurements are significant (P < 0.05) when compared to phenotypic and dietary controls.

Parameter	Lean		Obese	
	High Fat	Regular	High Fat	Regular
Estimated CEI (MJ/10 wk)	24.1 ± 3.3	24.5 ± 2.0	32.5 ± 4.0 [†]	35.1 ± 3.4 [†]
Change in Body Weight (g/10 wk)	80.4 ± 8.4	66.1 ± 2.4	148.9 ± 17.5 [†]	125.5 ± 11.3 [†]
Estimated EER ^a (g/MJ)	3.31 ± 0.23	2.71 ± 0.12	4.80 ± 0.43 ^{††}	3.53 ± 0.22 [†]
Final Body Weight (g)	289 ± 10	247 ± 4	445 ± 18 [†]	424 ± 21 [†]
Nasoanal length (cm)	21.2 ± 0.2	21.2 ± 0.2	21.9 ± 0.1 [†]	21.7 ± 0.3
Lee's index of obesity ^b	.301 ± .008	.295 ± .002	.350 ± .005 [†]	.347 ± .005 [†]
Heart Weight (mg)	914 ± 22	872 ± 32	1367 ± 76 ^{††}	1094 ± 25 [†]
Triglycerides (mg/dL)	141 ± 9	130 ± 12	2189 ± 538 [†]	2200 ± 946 [†]

Figure 3. Plasma leptin (O) and insulin (O) concentrations in lean control (LC), lean high fat (LHF), obese control (OC), and obese high fat (OHF) experimental groups after 10 weeks. *P < 0.05 vs. phenotypic controls. n=9 for lean groups and n=8 for obese groups. +P < 0.05 vs. dietary control.



Not Good

Summary

- On a standard diet, NO production by obese rats is greater than by lean rats.
- When obese rats are fed a high fat diet, NO production is markedly suppressed compared to obese rats on the diet of standard rat chow.
- Obese Zucker rats on a high fat diet develop hypertension when subjected to a salt load. In contrast, obese rats do not develop hypertension when subjected to the same salt load.
- Lean rats do not develop hypertension when subjected to the same experimental conditions that promote salt-sensitive hypertension in obese rats.

Conclusions

- Obesity is a risk factor for the development of salt sensitive hypertension.
- The suppression of NO production may promote the development of salt-sensitive hypertension in obese rats.

Acknowledgments

This research was supported in part by grant # P20 RR016477 from the National Center for Research Resources awarded to the West Virginia Biomedical Research Infrastructure Network and by the Marshall University Joan C. Edwards School of Medicine Cardiovascular Research Support Fund.

References

Bacon SL, Shenwood A, Hinderliter A, Blumenfeld JA. Effects of exercise, diet and weight loss on high blood pressure. *Sports Med*. 2004;34(5):307-16. Review. PMID: 15107009

Barnard RJ, Roberts CK, Varon GM, Berger J. Diet-Induced Insulin Resistance Precedes Other Aspects of the Metabolic Syndrome. *J Appl Physiol*. 1998 Apr;84(4):1311-5. PMID: 9516198

Brunner EK. Medical Aspects of Obesity. *Ann Intern Med* 1993; 119:655-663.

Vesely B. Dietary fat, fatty acid composition in plasma and the metabolic syndrome. *Curr Opin Lipidol*. 2003 Feb;14(1):159. Review. Abstract. PMID: 12544695

World Health Organization. *Obesity: Preventing and managing the global epidemic*. Report of a WHO Consultation: Geneva, 2000 (World Health Organization Technical Report Series; 894)

Not Good

Not Good

Good

Effective Posters

- ▣ Consider viewer impact
 - make it easy to read
 - make it easy to understand
 - people only have a few minutes per poster
- ▣ Keep it short, simple, and to the point

Effective Posters (cont.)

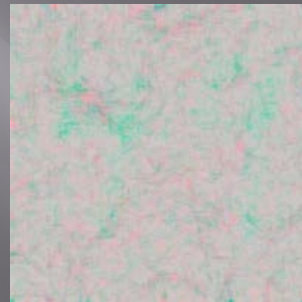
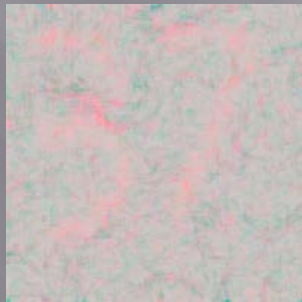
- ▣ Poster should be self-explanatory
 - remove all non-essential information
 - use verbal explanations to fill in the details
- ▣ Attract visual attention: use graphics
- ▣ Try for:
 - ▣ 25% text
 - ▣ 50% graphics
 - ▣ 25% empty space

Effective Posters (cont.)

- ▣ Pick one font and stick to it
 - use larger, bold, or italics font for emphasis
- ▣ Use bullet points rather than paragraphs
- ▣ If the title is too long, shorten it
 - don't reduce the font size

Effective Posters (cont.)

- ▣ Avoid red/green combinations
 - red/green color blindness is common



- ▣ Biggest mistake: too much text
 - the most effective posters provide minimal text

Effective Posters (cont.)

- ▣ A poster is not a research paper stuck to a board
 - avoid visual chaos
 - avoid shadowed text
 - make text easy to read
- ▣ View poster at 100%
 - text okay?
 - images pixilated?

Effective Posters (cont.)

- ▣ For poster approval...
 - be consistent!
 - ▣ not: Person #1, B.S., Person #2, PhD
 - ▣ not: “I would like to thank...”
 - ▣ ensure a 2” margin on the right hand side
 - ▣ one font throughout
 - ▣ paragraph indents – all the same
 - ▣ references in alphabetical order

 - be consistent!

Status of the West Virginia State Collection of Amphibians and Reptiles

Marshall University, Department of Biological Sciences, Huntington, WV 25755

Good

The West Virginia Academy of Science gave Neil D. Richmond \$100 in 1935 to travel the state and collect amphibians and reptiles. These specimens and supplemental collections in 1937 and 1938 formed the nucleus for a state collection of amphibians and reptiles. Since Richmond was not associated with a museum or university, he lacked curatorial services and a building to hold the collections. To provide curatorial services, the collections were moved to Marshall College in 1939 under the care of H. Bayard Green. H. B. Green maintained the collections from 1939 to 1971. During this time the collections grew from approximately 1,000 to over 5,000. Michael Seidel served as the curator from 1971 to 1987 and Thomas E. Pouley assumed the curatorship in 1987 and continues to provide curatorial services for the collection today. Presently, there are over 12,000 specimens. The West Virginia Division of Natural Resources, United States Park Service, and United States Department of Agriculture-Forest Service have provided financial assistance for the maintenance of the collections.

Research involving H. Bayard Green Museum of Natural History

(West Virginia Biological Survey)

- > 32 graduate students completed Master's theses
- > 13 current graduate students working on Master's theses
- > Many published research papers
- > Published book: Amphibians and Reptiles in WV (Green and Pouley 1987)
- > Work in progress: 2nd Edition of Amphibians and Reptiles in WV and WV Herpetological Atlas



Dr. N. Bayard Green

History of the West Virginia Biological Survey Collection

	Number of Known Species in West Virginia		Number of Specimens in Collection	
	1948	2003	1948	2003
Amphibians				
Salamanders	25	35	2,095	8,613
Freshwater Frogs	13	15	483	2,748
Subtotal	38	50	2,578	11,361
Reptiles				
Snakes	20	22	185	969
Lizards	5	6	77	312
Turtles	11	14	64	239
Subtotal	36	42	326	1,470
Total	74	92	3,107	12,781

Selected West Virginia Amphibians



Northern Red Salamander
Pseudotriton ruber



Northern Cricket Frog
Acris crepitans



Green Salamander
Aneides aeneus



Cope's Grey Treefrog
Hyla chrysoscelis



Four-toed Salamander
Hemidactylum scutum



Fowler's Toad
Bufo fowleri



Selected West Virginia Reptiles



Eastern Wormsnake
Carphophis a. amoenus



Common Snapping Turtle
Chelydra s. serpentina



Northern Red-bellied Snake
Storeria o. occipitmaculata



Wood Turtle
Clemmys insculpta



Black Ratsnake
Eliophis o. obsoleta



Northern Copperhead
Agkistrodon contortrix molaxianus

Acknowledgment

We thank the WVDNR and NPS for providing funding for the museum. Special thanks to all of the graduate and undergraduate students who have helped to build and maintain the museum. Photo by Mirrah Isakovich and Matt Watson.

Literature cited

Green, H.B. 1948. The Herpetological Collections of the West Virginia Biological Survey. West Virginia Academy of Science. 20:37-44.

PARENTAL PERCEPTION OF OVERWEIGHT/OBESE CHILDREN IN WV

Dept. of Pediatrics, Marshall University, Huntington, WV

Good

Abstract

Background: Twenty eight percent of low-income children between 2 and 5 years of age in West Virginia are overweight or at risk of becoming overweight (CDC, 2003). Previous studies have demonstrated that parents acknowledge the health risk of obesity, but medical interventions for obesity begin with the understanding of parental perception of the disease. **Objective:** To determine parental perception of obesity in West Virginia. **Design/Methods:** A questionnaire was given to parents in the pediatric outpatient clinic over a nine month period. Surveys were given to parents of children over 2 years of age. The survey contained questions about the appearance/appetite of their child and questions about the health related aspects of obesity. Overweight was defined as a BMI of 25 in adults and 85th percentile in children. Obesity was defined as a BMI 30 in adults and 95th percentile in children. **Results:** Of 400 surveys given, 344 were returned, of which 209 surveys had adequate data to be included. Overall, 120 (55%) parents and 69 (33%) children were overweight/obese (OW/OB). Of the 69 OW/OB children, a total of 49 (71%) were described as normal weight, and 50 (72%) were described as having a normal appetite. **Conclusions:** Most overweight/obese parents do not recognize obesity as a health problem, nor do they recognize obesity in their children. Future clinical guidelines to prevent obesity must acknowledge parental attitudes and perception of the problem.

Methods

SURVEY QUESTIONS

Do you think your child is: underweight/normal weight/overweight

Do you think your child's appetite is: too little/just right/too much

Do you think obesity is a health problem?

Do you think obesity is preventable?

Do you think that children who are obese grow up to be obese adults?

Rank how important these factors are to making someone overweight:
emotional stress
genetics
lack of exercise
overeating
type of foods eaten

Does your child's Doctor speak with you about nutrition?

If yes, how much?
too little/just right/too much

If no, would you like your child's Doctor to speak with you about nutrition at routine visits?

Rank these sources by information concerning nutrition:
books newspaper
doctor television
friends/family WIC
internet magazines
Other

Do you struggle with your weight?

Results

Parents:



Children:



Of the overweight/obese children, 71% were described by parents as being of normal weight and 72% were described as having a normal appetite.

Overweight/obese children (n = 69)

	OW/OB Parent	NW Parent	P-value
Perceived as NW	33 (60%)	16 (33%)	0.211
Appetite described as just right	31 (60%)	15 (30%)	0.211

Parents were asked to comment on the health related aspects of obesity:

Is obesity a health problem?
20% answered No (63% OW/OB)

Is obesity preventable?
8% answered No (73% OW/OB)

Do obese children grow up to be obese adults?
23% answered No (48% OW/OB)

Overeating ranked as #1 factor involved in making someone overweight

75% stated physician spoke with them about their child's nutrition

Doctor ranked as #1 source of nutrition information

54% stated they struggle with their weight

Conclusion

In our population, 55% of parents and 33% of children were obese or overweight

The majority of parents did not recognize obesity in their child

Obese/overweight parents are not more likely than normal weight parents to fail to recognize that their child is overweight/obese

However, most overweight/obese parents do not recognize obesity as a health problem

Future clinical guidelines in obesity prevention must acknowledge parental attitudes and perception of the problem

References

www.cdc.gov



SEM IMAGING OF THE SENSORY ORGAN, CAMPANIFORM SENSILLAE, OF WILD-TYPE AND MUTANTS OF THE FRUIT FLY, *Drosophila melanogaster*.

Dept. of Biological Sciences, Marshall University

Good

ABSTRACT

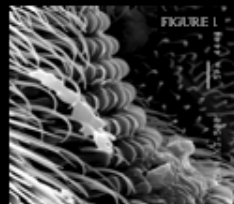
The sense organs are specialized epidermal structures for the reception of external stimuli such as contact vibrations, taste, odor, and light. There are different types of sense organs that the fruit fly utilizes, however, this experiment focuses on just one type. The campaniform sensilla (CS) are dome shaped sense organs found on three different body parts of the *Drosophila*, the halteres, the leg, and the wing. The focus of the research was aimed at the halteres CS. Two different phenotypes of fruit flies were examined in this experiment a wild type (Oregon R) and a mutant (*prickle*). The CS on the halteres of both flies were examined by imaging halteres via the SEM microscope. The images were examined to determine if there was a difference in the orientation of the haltere CS between the wild type and *prickle* mutant fly. The images were viewed and studied and it was found that there was a slight similarity in orientations of the CS between the two types of flies. Continued research will be beneficial to further the findings in this area of emphasis.



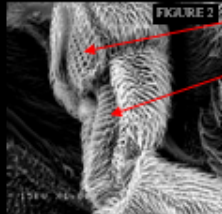
The arrows show a pedicel that leads from the haltere to the bristles.

INTRODUCTION

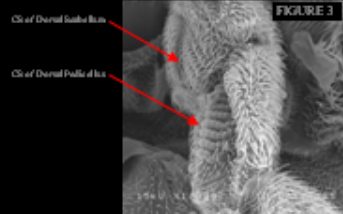
The epidermis of the adult *Drosophila* is patterned with many sense organs including the light-sensitive ommatidia of the compound eye and the mechanosensory bristles. Both ommatidia and bristles have a specific orientation or polarity that's consistent from fly to fly and which is assumed to be functionally important. This polarity requires the activity of the Planar Cell Polarity (PCP) genes during the development of the sense organs, and mutations in these genes cause the irregular orientation of ommatidia and bristles. A third class of sense organs are the campaniform sensilla (CS) that are present at the specific locations on the halteres, leg, and wings. Although the *Drosophila* CS have previously been characterized by the Scanning Electron Microscope (SEM), little has been described about the underlying polarity and the genetic mechanisms required for their orientation. The aim of this study is to use the SEM to investigate differences in CS orientation between wild type flies and flies mutant for the PCP genes.



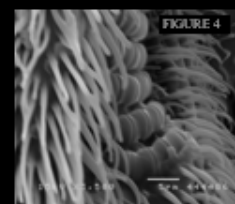
Wild type (Oregon R) ventral pedicellar CS



Oregon R CS of dorsal Pedicellum and Scalellum of Haltere



prickle CS of dorsal Pedicellum and Scalellum of Haltere



Mutant (prickle) ventral pedicellar CS

Images obtained by Anton Smith and David Neff.

MATERIALS AND METHODS

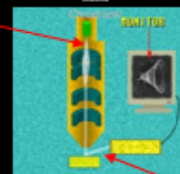
During the course of this research I was involved with using the SEM to obtain my images of the haltere CS. The SEM is a microscope that allows one to obtain very detailed images of microscopic materials by way of an electron beam scanning the surface of the specimen and projecting the image on a TV screen (below is a brief overview of how the SEM works). Preparation for my samples involved dissecting parts of the flies, including the leg and wings, to obtain what needed views of the halteres. Once the flies were mounted on metal stubs for SEM samples, sputter coating was essential before viewing through the SEM. This allows for the sample to be able to conduct electricity because the specimens are illuminated with electrons when being viewed. The use of a fixation method (described below, right) was necessary to decrease the shrinking that took place during the sputter coating and also within the vacuum of the SEM. This allowed for the images to not have a shriveled, impactive appearance when viewing, helping to maintain the 3-D structure. Viewing the images was then done on the computer after pictures were taken of the images that were obtained on the microscope. This image set was Oregon R wild type and flies homozygous for the *prickle* gene allele *prickle#440*.



RESULTS AND DISCUSSION

The purpose of this research was to determine if the mutant fly CS orientations were different from the wild type fly. There are three different sections of the haltere, the pedicellum (innermost section), the pedicellum (mid section), and the Capitellum (outermost section). The fields of CS that were studied in this experiment were located on the scalellum and pedicellum. I found that there was a large difference in the CS on the dorsal pedicellum, which is apparent in Figure 2 and Figure 3. The number of CS on the mutant fly are disoriented and not in line as they should be (see Fig. 2). The spacing between the rows of the pedicellar CS on the mutant fly also had wider than on the wild type fly. However, on the same figures (2 & 3) the dorsal CS on the scalellum had similar in orientation. Also, apparent in Figures 1 & 4, the ventral pedicellar CS are not altered as well. Some errors could have also occurred during the research as well. These could have also been a fault in the fixation methods since they were kept in separate vials when going through the process, which could have caused some error. Further research and imaging would be very helpful in making the determination that the *prickle* gene aids in altering orientation of the dorsal pedicellar CS.

Electron Beam
Electrons shoot down a tunnel through an array of magnetic lenses that focus the beam on a spot (specimen).



The detector first counts the electrons and the amplifier receives the signals that eventually are processed into an image on the monitor.

Secondary electrons are knocked loose from the specimen's surface and sent to the detector and amplifier.

Standard Chemicals/lysis Fixation

The 8 ml vial consisted of: 10 ml 25% glutaraldehyde
50 ml buffer stock solution cacodylate buffer, pH 7.3-7.4
Make up 100 ml's with distilled water
Final Concentration: 2.5% glutaraldehyde in 0.1 M sodium cacodylate
During fixation I transferred the flies in to vials for approximately 8-12 hrs rotating the flies in vials. I then rinsed the flies overnight in the buffer solution. I then rinsed flies in water and processed onto the final step in the method, the dehydration of alcohol series. The alcohol series consisted of first of the flies in different percentages of ethanol (5ml series in each of 60, 70, 80%, 90%, 100%, & 100%) (Final Concentration is used twice and also for approximately 30 ml).

CHARACTERIZATION OF PLANT CELL BIOMASS AND BIOPRODUCT PRODUCTION IN A MICROGRAVITY-BASED HYDRODYNAMIC FOCUSING BIOREACTOR (HFB)

Department of Biological Sciences, Marshall University, Huntington, WV 25755, NASA/Johnson Space Center, 2101 NASA Road 1, Mail code: S J, Houston, TX 77058-3696

ABSTRACT
 The purpose of this study was to evaluate the growth and bioproduction of plant cell biomass in a microgravity-based hydrodynamic focusing bioreactor (HFB). The HFB was used to culture plant cells under microgravity conditions, and the resulting biomass was analyzed for growth and bioproduction. The HFB was found to be a suitable bioreactor for the culture of plant cells, and the resulting biomass was found to be suitable for bioproduction. The HFB was found to be a suitable bioreactor for the culture of plant cells, and the resulting biomass was found to be suitable for bioproduction.

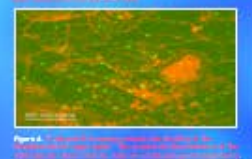


Figure 1. Photograph of the HFB bioreactor.

Figure 2. Photograph of the HFB bioreactor.

Figure 3. Schematic diagram of the HFB system.

Figure 4. Flowchart of the HFB system.

Figure 5. Schematic diagram of the HFB system.

Figure 6. Photograph of the HFB bioreactor.

Figure 7. Photograph of the HFB bioreactor.

Figure 8. Photograph of the HFB bioreactor.

Figure 9. Photograph of the HFB bioreactor.

Figure 10. Photograph of the HFB bioreactor.

Figure 11. Photograph of the HFB bioreactor.

Figure 12. Photograph of the HFB bioreactor.

Figure 13. Photograph of the HFB bioreactor.

Figure 14. Photograph of the HFB bioreactor.

Figure 15. Photograph of the HFB bioreactor.

Figure 16. Photograph of the HFB bioreactor.

Figure 17. Photograph of the HFB bioreactor.

Figure 18. Photograph of the HFB bioreactor.

Figure 19. Photograph of the HFB bioreactor.

Figure 20. Photograph of the HFB bioreactor.

Figure 21. Photograph of the HFB bioreactor.

Figure 22. Photograph of the HFB bioreactor.

Figure 23. Photograph of the HFB bioreactor.

Figure 24. Photograph of the HFB bioreactor.

Figure 25. Photograph of the HFB bioreactor.

Figure 26. Photograph of the HFB bioreactor.

Figure 27. Photograph of the HFB bioreactor.

Figure 28. Photograph of the HFB bioreactor.

INTRODUCTION

The purpose of this study was to evaluate the growth and bioproduction of plant cell biomass in a microgravity-based hydrodynamic focusing bioreactor (HFB). The HFB was used to culture plant cells under microgravity conditions, and the resulting biomass was analyzed for growth and bioproduction. The HFB was found to be a suitable bioreactor for the culture of plant cells, and the resulting biomass was found to be suitable for bioproduction.



Figure 29. Micrograph showing plant cell biomass in the HFB.



Figure 30. Micrograph showing plant cell biomass in the HFB.

Figure 31. Micrograph showing plant cell biomass in the HFB.

Figure 32. Micrograph showing plant cell biomass in the HFB.

The purpose of this study was to evaluate the growth and bioproduction of plant cell biomass in a microgravity-based hydrodynamic focusing bioreactor (HFB). The HFB was used to culture plant cells under microgravity conditions, and the resulting biomass was analyzed for growth and bioproduction. The HFB was found to be a suitable bioreactor for the culture of plant cells, and the resulting biomass was found to be suitable for bioproduction.



Figure 33. Photograph of the HFB bioreactor.

Figure 34. Photograph of the HFB bioreactor.

Figure 35. Photograph of the HFB bioreactor.

Figure 36. Photograph of the HFB bioreactor.

Figure 37. Photograph of the HFB bioreactor.

Figure 38. Photograph of the HFB bioreactor.

Figure 39. Photograph of the HFB bioreactor.

Figure 40. Photograph of the HFB bioreactor.

Figure 41. Photograph of the HFB bioreactor.

Figure 42. Photograph of the HFB bioreactor.

Figure 43. Photograph of the HFB bioreactor.

Figure 44. Photograph of the HFB bioreactor.

Figure 45. Photograph of the HFB bioreactor.

Figure 46. Photograph of the HFB bioreactor.

Figure 47. Photograph of the HFB bioreactor.

Figure 48. Photograph of the HFB bioreactor.

Figure 49. Photograph of the HFB bioreactor.

Figure 50. Photograph of the HFB bioreactor.

Figure 51. Photograph of the HFB bioreactor.

Figure 52. Photograph of the HFB bioreactor.

Figure 53. Photograph of the HFB bioreactor.

Figure 54. Photograph of the HFB bioreactor.

Figure 55. Photograph of the HFB bioreactor.

Figure 56. Photograph of the HFB bioreactor.

Figure 57. Photograph of the HFB bioreactor.

Figure 58. Photograph of the HFB bioreactor.

Figure 59. Photograph of the HFB bioreactor.

Figure 60. Photograph of the HFB bioreactor.

Figure 61. Photograph of the HFB bioreactor.

Figure 62. Photograph of the HFB bioreactor.

Figure 63. Photograph of the HFB bioreactor.

Figure 64. Photograph of the HFB bioreactor.

Figure 65. Photograph of the HFB bioreactor.

Figure 66. Photograph of the HFB bioreactor.

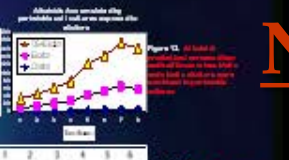


Figure 67. Line graph showing biomass production over time.

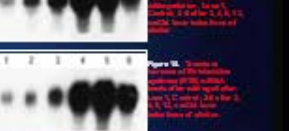


Figure 68. Gel electrophoresis image showing protein bands.

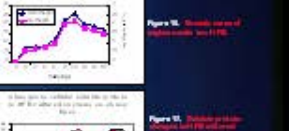


Figure 69. Line graph showing biomass production over time.



Figure 70. Line graph showing biomass production over time.



Figure 71. Gel electrophoresis image showing protein bands.



Figure 72. Line graph showing biomass production over time.



Figure 73. Line graph showing biomass production over time.



Figure 74. Gel electrophoresis image showing protein bands.

Not Good

Figure 29. Micrograph showing plant cell biomass in the HFB.

Figure 30. Micrograph showing plant cell biomass in the HFB.

Figure 33. Photograph of the HFB bioreactor.

Figure 67. Line graph showing biomass production over time.

Not Good



NASA Scholar Recipient



PROGESTIN STIMULATION OF MANGANESE SUPEROXIDE DISMUTASE

IN T47D HUMAN BREAST CANCER CELLS

Departments of Biochemistry and Microbiology and Pharmacology, Physiology, and Toxicology¹,
Joan C. Edwards School of Medicine, Marshall University, Huntington, WV



Abstract

11- β Testosterone propionate (TP) has been shown to increase the rate of proliferation of the progestin-responsive (PR+) T47D human breast cancer cell line. The present study explored the possibility that the stimulation by TP of cell growth is mediated by an increase in the rate of synthesis of the antioxidant enzyme manganese superoxide dismutase (MnSOD) as one of the dependent variables. A 24 hr treatment of T47D cells with TP (10⁻⁶ M) increased MnSOD activity 10-fold when measured by immunoblotting. This increase was blocked by the MnSOD inhibitor diethylthiocarbamate (DETCA) and by the MnSOD promoter inhibitor, 1- α -25-dihydroxyvitamin D₃ (1,25-D₃). The effect of TP on MnSOD activity was also blocked by the protein synthesis inhibitor cycloheximide (CHX). The effect of TP on MnSOD activity was also blocked by the protein synthesis inhibitor cycloheximide (CHX). The effect of TP on MnSOD activity was also blocked by the protein synthesis inhibitor cycloheximide (CHX).

Introduction

Superoxide anion (O₂⁻) is a naturally occurring anionic oxidant for activation of apoptosis (1). It is also produced by the active transport of iron into the mitochondria (2). The following reactions are involved in the production of O₂⁻:

$$2O_2 + 2H^+ \rightleftharpoons H_2O_2 + O_2 \quad A$$

$$2H_2O_2 \rightleftharpoons O_2 + 2H_2O \quad B$$

$$GSH + ROOH \rightleftharpoons GSSG + H_2O + ROH \quad C$$

Figure 1. Chemical reactions in the production of superoxide.

Superoxide anion is a naturally occurring anionic oxidant for activation of apoptosis (1). It is also produced by the active transport of iron into the mitochondria (2). The following reactions are involved in the production of O₂⁻:

Superoxide anion is a naturally occurring anionic oxidant for activation of apoptosis (1). It is also produced by the active transport of iron into the mitochondria (2). The following reactions are involved in the production of O₂⁻:

Superoxide anion is a naturally occurring anionic oxidant for activation of apoptosis (1). It is also produced by the active transport of iron into the mitochondria (2). The following reactions are involved in the production of O₂⁻:

Superoxide anion is a naturally occurring anionic oxidant for activation of apoptosis (1). It is also produced by the active transport of iron into the mitochondria (2). The following reactions are involved in the production of O₂⁻:

Superoxide anion is a naturally occurring anionic oxidant for activation of apoptosis (1). It is also produced by the active transport of iron into the mitochondria (2). The following reactions are involved in the production of O₂⁻:

Experimental

Cell Culture. T47D human breast cancer cells were grown in the presence of 10% fetal bovine serum (FBS) in DMEM supplemented with 10% FBS. Cells were grown in the presence of 10% FBS in DMEM supplemented with 10% FBS. Cells were grown in the presence of 10% FBS in DMEM supplemented with 10% FBS.

Western Blot Analysis. Cells were grown in 10% FBS in DMEM supplemented with 10% FBS. Cells were grown in the presence of 10% FBS in DMEM supplemented with 10% FBS. Cells were grown in the presence of 10% FBS in DMEM supplemented with 10% FBS.

MnSOD Activity Assay. Cells were grown in 10% FBS in DMEM supplemented with 10% FBS. Cells were grown in the presence of 10% FBS in DMEM supplemented with 10% FBS. Cells were grown in the presence of 10% FBS in DMEM supplemented with 10% FBS.

Experimental (continued)

Western Blot Analysis. Cells were grown in 10% FBS in DMEM supplemented with 10% FBS. Cells were grown in the presence of 10% FBS in DMEM supplemented with 10% FBS. Cells were grown in the presence of 10% FBS in DMEM supplemented with 10% FBS.

Results

A 24 hr treatment of T47D cells with TP (10⁻⁶ M) increased MnSOD activity 10-fold when measured by immunoblotting. This increase was blocked by the MnSOD inhibitor DETCA and by the MnSOD promoter inhibitor, 1- α -25-dihydroxyvitamin D₃ (1,25-D₃).

A 24 hr treatment of T47D cells with TP (10⁻⁶ M) increased MnSOD activity 10-fold when measured by immunoblotting. This increase was blocked by the MnSOD inhibitor DETCA and by the MnSOD promoter inhibitor, 1- α -25-dihydroxyvitamin D₃ (1,25-D₃).

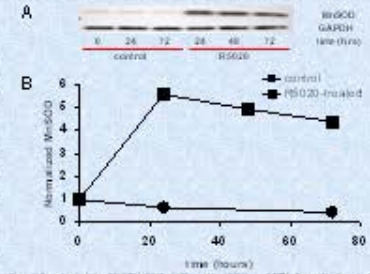


Figure 2. Western blot analysis of MnSOD and GAPDH levels in control and progesterone-treated T47D cells at 0, 12, 24, and 48 hours. MnSOD levels increase significantly with progesterone treatment.

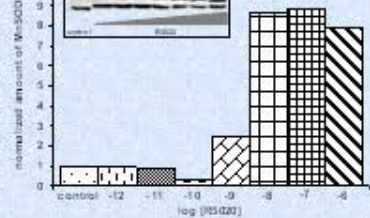


Figure 3. Bar graph showing normalized MnSOD activity in control and progesterone-treated T47D cells at various time points. Activity increases significantly with progesterone treatment.

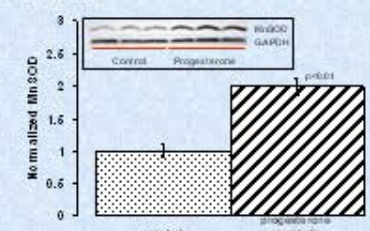


Figure 4. Western blot analysis of MnSOD and GAPDH levels in control and progesterone-treated T47D cells. MnSOD levels increase significantly with progesterone treatment.

Results (continued)

Table 1: Progesterone stimulation of MnSOD activity in T47D cells. The table shows MnSOD activity (pmol/min/mg protein) for control and progesterone-treated cells at various time points (0, 12, 24, 48 hours).

Table 1. Progesterone stimulation of MnSOD activity in T47D cells. MnSOD activity (pmol/min/mg protein) is shown for control and progesterone-treated cells at 0, 12, 24, and 48 hours. Activity increases significantly with progesterone treatment.

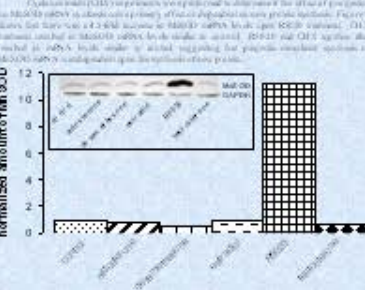


Figure 5. Stacked bar graph showing MnSOD activity in control and progesterone-treated T47D cells at 0, 12, 24, and 48 hours. Activity increases significantly with progesterone treatment.

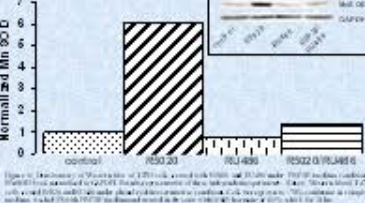


Figure 6. Bar graph showing MnSOD activity in control and progesterone-treated T47D cells at 0, 12, 24, and 48 hours. Activity increases significantly with progesterone treatment.

Discussion

The present study demonstrates that 11- β testosterone propionate (TP) increases the rate of synthesis of the antioxidant enzyme manganese superoxide dismutase (MnSOD) in T47D human breast cancer cells. This increase is blocked by the MnSOD inhibitor DETCA and by the MnSOD promoter inhibitor, 1- α -25-dihydroxyvitamin D₃ (1,25-D₃).

The present study demonstrates that 11- β testosterone propionate (TP) increases the rate of synthesis of the antioxidant enzyme manganese superoxide dismutase (MnSOD) in T47D human breast cancer cells. This increase is blocked by the MnSOD inhibitor DETCA and by the MnSOD promoter inhibitor, 1- α -25-dihydroxyvitamin D₃ (1,25-D₃).

Discussion (continued)

The present study demonstrates that 11- β testosterone propionate (TP) increases the rate of synthesis of the antioxidant enzyme manganese superoxide dismutase (MnSOD) in T47D human breast cancer cells. This increase is blocked by the MnSOD inhibitor DETCA and by the MnSOD promoter inhibitor, 1- α -25-dihydroxyvitamin D₃ (1,25-D₃).

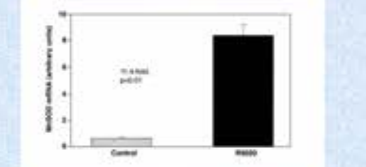


Figure 7. Bar graph showing MnSOD activity in control and progesterone-treated T47D cells. Activity increases significantly with progesterone treatment.

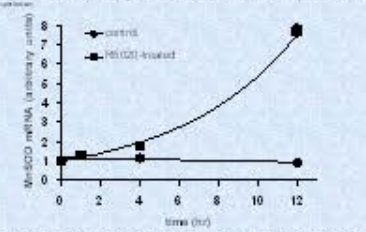


Figure 8. Line graph showing MnSOD activity in control and progesterone-treated T47D cells over time. Activity increases significantly with progesterone treatment.

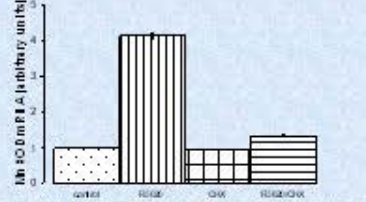


Figure 9. Bar graph showing MnSOD activity in control and progesterone-treated T47D cells at 0, 12, 24, and 48 hours. Activity increases significantly with progesterone treatment.

Conclusions

- 1. Progesterone stimulates MnSOD synthesis in T47D human breast cancer cells in a dose-dependent manner.
- 2. This effect is specific for progesterone. The effect of other steroid hormones on MnSOD synthesis is not observed.
- 3. The effect of progesterone on MnSOD synthesis is blocked by the MnSOD inhibitor DETCA and by the MnSOD promoter inhibitor, 1- α -25-dihydroxyvitamin D₃ (1,25-D₃).

Acknowledgements

The authors thank Dr. J. Douglas for his helpful suggestions during the course of this study.

References

- 1. Halliwell B. Superoxide anion and its role in oxidative stress. *J Biochem Sci* 1991;16:1-14.
- 2. Halliwell B. Superoxide anion and its role in oxidative stress. *J Biochem Sci* 1991;16:1-14.
- 3. Halliwell B. Superoxide anion and its role in oxidative stress. *J Biochem Sci* 1991;16:1-14.

Not Good

Questions?



References

- <http://www.biology.lsa.umich.edu/research/labs/ktosney/file/PostersHome.html>
- <http://www.ncsu.edu/project/posters/GoodGraphs>
- <http://projects.cs.dal.ca/DCSI/present.ppt#1>
- <http://www.cmer.wsu.edu/~yonge/ce465/poster.pdf>
- <http://depts.washington.edu/mphpract/perfect%20Poster.ppt#1>
- http://www.asp.org/education/howto_onPosters.html